Chinese Science Bulletin

Phase field simulation of monotectic transformation for liquid Ni-Cu-Pb alloys

LUO BingChi, WANG HaiPeng & WEI BingBo†

Department of Applied Physics, Northwestern Polytechnical University, Xi'an 710072, China

Based on the subregular solution model, the liquid phase separation of ternary $(Ni_xCu_{100-x})_{50}Pb_{50}$ monotectic alloys is simulated by the phase field method. It is found that if the surface segregation potential is not incorporated, the dynamic morphologies of alloy melt show a transition from disperse microstructure into bicontinuous microstructure with the increase of fluidity parameter. When the surface segregation potential is coupled, Pb-rich phase migrates preferentially to the surface of the liquid alloy, and the Ni-rich phase depends on the Pb-rich phase to nucleate. With the extension of the phase separation time, the surface layer is formed through coagulation and growth, and its thickness gradually increases. The Ni-rich phase migrates to the central part, and finally a two-layer core-shell microstructure is produced. The concentration in the surface layer fluctuates more conspicuously than that inside the bulk phase, which subsequently transfers from the surface to the interior by a wave. The fluid field near the liquid-liquid interface is strong at the beginning of phase separation, and reduces later on. The surface segregation is essential to the formation of the surface layer, concentration profile variation, fluid field distribution and phase separation morphology.

phase separation, surface segregation, phase field simulation, monotectic alloy

Liquid phase separation of monotectic alloys has become a major research field within material physics[1,2]. For liquid metals, the solidification process is difficult to observe *in situ*. Therefore, it is studied only by analyzing solidification microstructure. Unfortunately, the morphology evolution of alloy melt before solidification is not directly obtainable. In recent years, the phase field method has been sufficiently developed, which provides a novel access to investigating various evolution processes and phase separation behaviors[3]. Previously, Tanaka[4] explored the interplay between wetting and phase separation for organic mixtures using the phase field model, and found that hydrodynamics plays an important role in bicontinuous phase separation. Afterwards, Bhagavatula and Jasnow[5] investigated the influence of Marangoni migration on phase separation. In principle, Marangoni migration originates from the melt temperature gradient, which drives the second liquid phase towards the higher temperature region. The Marangoni migration of droplets is restrained under normal gravity conditions, whereas it becomes conspicuous under microgravity conditions. Huo et al.[6] further considered the chemical reaction for a binary mixture and studied phase separation with hydrodynamic effects based on Model H[7]. The phase field method has been extensively applied in many fields. Investigation of phase separation involves many interdisciplinary subjects, such as hydrodynamics, materials physics and chemistry. Thus, it is very difficult to study phase separation.

Up to now, theoretical investigation of phase separation mainly focuses on high molecular weight polymers[8,9], water[10], water-oil-surfactants[11], bilayer lipid membranes[12] and lysozymes[13]. Experimental studies[2,14,15] on phase separation extend to ternary alloys,

Received July 2, 2008; accepted September 22, 2008
doi: 10.1007/s11434-009-0018-5
†Corresponding author (email: bbwei@nwpu.edu.cn)
Supported by the National Natural Science Foundation of China (Grant Nos. 50121101, 50395105)

which mainly explores the phase separation mechanism by analyzing solidified microstructures. Due to the opacity of alloy melt, it is difficult to observe the phase separation route in the experiment. Nevertheless, numerical simulation reveals the phase separation process. Experimental investigations on alloy melt for phase separation are frequently reported. By contrast, theoretical analysis on alloy melt for phase separation are still scarce, especially for ternary monotectic alloys. The objective of this work is to investigate the phase separation for ternary $(Ni_xCu_{100-x})_{50}Pb_{50}$ monotectic alloys using the phase field method, which is extended by coupling the surface segregation, fluid field and temperature field. Furthermore, the effect of surface segregation on phase separation is studied, and the formation of a segregation layer, the concentration profile variation and fluid field distribution are discussed.

1 Phase separation model

The elements Ni and Cu infinitely dissolve each other and form a binary isomorphous system. Usually, the solidified microstructures of ternary Ni-Cu-Pb monotectic alloy consist of (Ni,Cu) and (Pb) phases. Ni and Cu elements are viewed as one component, and the ternary Ni-Cu-Pb monotectic alloy is investigated as a pseudobinary system.

According to the second law of thermodynamics, the system always evolves towards the state with lower energy. Once the temperature of a ternary Ni-Cu-Pb monotectic alloy is below the immiscible liquidus surface, the phase separation will take place to reduce the total energy. The decrease of Gibbs free energy is the driving force of phase separation.

Alloy melt consists of two components A and B with molar fractions $x_A=\phi$ and $x_B=1-\phi$. A is the (Ni,Cu) pseudo component and B is the Pb component. The bulk Gibbs free energy is described by the following subregular solution model[16]:

$$G_b = g_A x_A + g_B x_B + RT[\phi\ln\phi + (1-\phi)\ln(1-\phi)] + RT_c\Omega\phi(1-\phi), \quad (1)$$

where g_A and g_B are the Gibbs free energy of A and B. R is the gas constant, T_c the critical temperature and Ω the interaction coefficient between two species A and B.

As soon as the liquid phase separation occurs, the liquid-liquid interface will come into being. Hence, the melt energy will be changed. Cahn and Hilliard[17] proposed the free energy functional $F(\phi)$ to describe it, which is expressed as

$$F(\phi) = \int \mathrm{d}V\left[G_b + \frac{1}{2}RT_c\varepsilon^2(\nabla\phi)^2\right], \quad (2)$$

where ε is the characteristic microscopic length. The chemical potential is defined as

$$\mu = \frac{\delta F}{\delta\phi} = \frac{\partial F}{\partial\phi} - \nabla\frac{\partial F}{\partial(\nabla\phi)}, \quad (3)$$

where T_c is set as the temperature scale, ε as the length scale and RT_c as the energy scale. In terms of eqs. (2) and (3), the dimensionless chemical potential is derived as

$$\tilde{\mu} = \mu_0 + \theta\ln\left(\frac{\phi}{1-\phi}\right) + \Omega(1-2\phi) - \nabla^2\phi, \quad (4)$$

where $\mu_0=(g_B-g_A)/RT$, and the reduced temperature $\theta=T/T_c$. The phase field equation is written by Model H[7]:

$$\frac{\partial\phi}{\partial t} + \nabla\cdot(v\phi) = -\nabla\cdot\left[\phi(1-\phi)\nabla\tilde{\mu}\right] + \nabla\cdot\xi, \quad (5)$$

where ξ is the random Gaussian white noise, the fluctuation amplitude is the unit and the mean value is zero. The fluid field equation is simplified as[18]

$$v = -C_f\phi\nabla\mu, \quad (6)$$

where C_f is the fluidity parameter of alloy melt, $C_f = \rho RT_c\varepsilon^2/6\pi D_L\eta M$, and the greater it becomes, the more quickly the flow field responds to the local force field. ρ is the mass density, D_L is the diffusion coefficient, η is the viscosity, and M is the molar weight.

In order to include the temperature field effect, the dimensionless temperature field is given as

$$\frac{\partial\theta}{\partial\tau} = \frac{\alpha}{D_L}\nabla^2\theta, \quad (7)$$

where α is the thermal diffusion coefficient.

The extended Model H simulates the phase separation of the binary alloy[18]. In the light of the different systems, the phenomenological model introduced into the modified item describes the evolutionary characteristics of alloy melt. If the free surface effect is taken into account in the studied object, eq. (2) introduces the surface free energy $V(z)$. Here, $V(z)=0.8$, $z\leqslant 1$ near the surface; $V(z)=0.8/z^4$, $z>1$ far from the surface[16]. In addition, eqs. (5)—(7) are supplemented by proper boundary conditions at the surface. The Neumann boundary condition is employed for the concentration field, i.e. $\boldsymbol{n}\cdot\nabla\phi=0$, where $\boldsymbol{n}$ denotes the normal direction at the surface.

Other boundary conditions are no flux for the temperature field $\boldsymbol{n}\cdot\nabla\theta=0$, and no slip for the velocity field $\boldsymbol{n}\cdot\nabla\boldsymbol{v}=0$.

2 Results and discussion

The governing eqs. (4)—(7) are solved on a uniform two dimensional square grid by an explicit finite difference technique. The time and space integration is calculated with a forward difference scheme and a center difference scheme. While time step $\Delta\tau$ and space step Δx satisfy $\Delta\tau/\Delta x^2 \leqslant D_L/(4\alpha)$, numerical calculations of eqs. (5) and (7) are convergent and stable. In our simulations, the initial molar concentration of Pb $\phi_0=0.5$, and the initial velocity were zero. The noise amplitudes of both the phase field and the temperature field were 0.015, and the grid sizes $\Delta x=\Delta y=1$. The time step $\Delta\tau=0.001$ ensures the stability of the numerical solution. The codes are written in the FORTRAN language, and the calculations were performed by a Lenovo 1800 cluster system.

In order to test the validity and accuracy of the calculation method, the morphology evolution was simulated without a fluid field, as shown in Figure 1(a). In such a case, Puri and Binder[1] also investigated the phase separation morphologies, whose results have been accepted by many researchers. The close agreement between our calculated result and ref. [1] suggests the accuracy and stability of the calculated program.

To explore the influence of fluid field and surface segregation on phase separation, a simplified case was initially considered. The temperature difference of inner melt is sufficiently small that the surface free energy is negligible. In such a case, it is regarded as the morphology evolution of the bulk phase. During the simulation, the composition of alloy melt is $(Ni_xCu_{100-x})_{50}Pb_{50}$, and the molar fraction of Ni and Cu element is an arbitrary ratio. The fixed lattice size is set as 1000×1000. Phase separation evolution is simulated with different fluidity parameters C_f. Figure 1 consists of four snapshots at 15 ms, which correspond to the respective fluidity parameters of 0, 10, 100 and 1000 from the morphology of Figure 1(a) and (b). When the fluid field is weak, i.e. the fluidity parameters are generally below 100, the white (Ni,Cu) phase uniformly distributes within the black Pb-rich phase in the form of spherical droplets. (Ni,Cu) phase droplets grow and coarsen after phase separation, and the average diameter of spheres in Figure 1(b) is larger than that in Figure 1(a). This indicates that the fluid field accelerates the coagulation of droplets. Additionally, the white (Ni,Cu) phase distributes within the black Pb-rich phase with bicontinuous microstructure, as illustrated in Figure 1(c) and (d). Owing to the rapid response of the fluid field, the solute diffusion is facilitated. The evolution morphology is mainly characterized by a bicontinuous microstructure. Tanaka[4] concluded that the hydrodynamic effect is an important factor to drive the phase separation. Evidently, if the surface segregation is not incorporated, the dynamic morphologies of alloy melt show a transition from disperse microstructure into bicontinuous microstructure with the increase of the fluidity parameter.

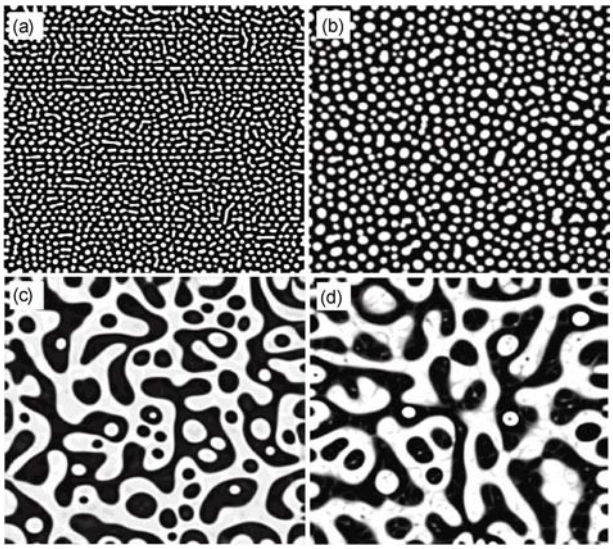

Figure 1 Snapshots from the microstructural evolution process with different fluidity parameters. (a)—(d) correspond to fluidity parameters of 0, 10, 100 and 1000. The equilibrium concentration $\phi_0=0.5$, and the grey level varies linearly between black and white. The white phase is (Ni,Cu) and the black area is (Pb).

Bažec and Žumer[9] found that the surface effect has a great influence on phase separation. In our model, the surface free energy is logically considered. The composition of alloy remains $(Ni_xCu_{100-x})_{50}Pb_{50}$, and the fluidity parameter $C_f=1000$. The lattice size in the square region is 400×400. Figure 2 presents the different morphologies of monotectic alloy, which correspond to phase separation time of 15 ms and 45 ms. At the beginning of phase separation, the Pb-rich phase migrates preferentially to the surface of the liquid alloy, while the (Ni,Cu) phase nucleates depending on the Pb-rich phase, as seen in Figure 2(a). With the increase of phase separation time, the thickness of the surface layer gradually

increases. The (Ni,Cu) phase is gradually formed and coarsened, which randomly distributes within the Pb-rich phase in a spherical manner, as illustrated in Figure 2(b). The calculated results indicate that the Pb-rich phase migrates preferentially to the surface of the liquid alloy. The surface segregation has a striking influence on phase separation.

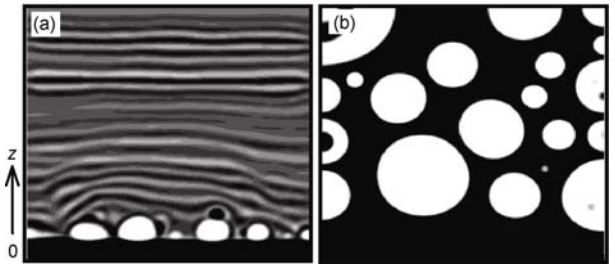

Figure 2 Influence of surface segregation on phase separation. Pb concentration ϕ_0=0.5 and fluidity parameter C_f=1000. The black phase is (Pb) and the white phase is (Ni,Cu). (a) and (b) correspond to 15 ms and 45 ms.

Figure 3 gives the concentration profiles of the vertical surface at 15 ms, 25 ms, 35 ms and 45 ms. It is apparent that the Pb concentration in the surface layer fluctuates more drastically than that inside the bulk phase, which subsequently transfers from the surface to the interior by a wave along the z direction. With the extension of phase separation time, the concentration fluctuation sharply increases. The wave crest and wave trough become flat and broad. The peak height decreases and the plateau becomes wider, which indicates that the droplets of the (Ni,Cu) phase coarsen and grow. Therefore surface segregation is the driving force of phase separation.

Once the fluid field is incorporated, the segregation layer becomes rough. For further investigation of the growth law of surface layers, the average thickness d_a denotes the ratio of the Pb-rich phase area to the length. Figure 4 shows the relationship between the thickness of the segregation layer and the phase separation time. With the increase of phase separation time, the thickness of Pb-rich phase gradually increases. Surface segregation is the driving force of segregation layer growth.

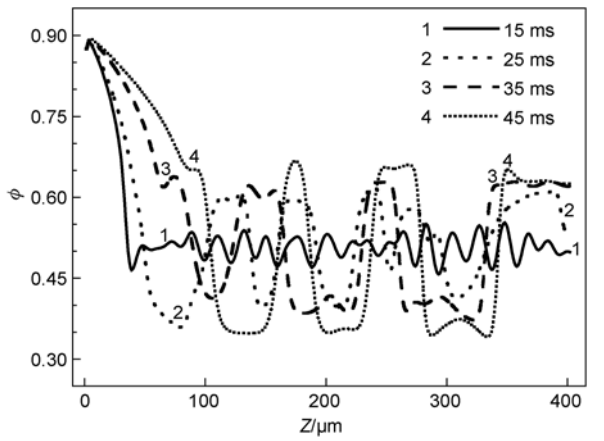

Figure 3 Concentration variation in the z direction at different time.

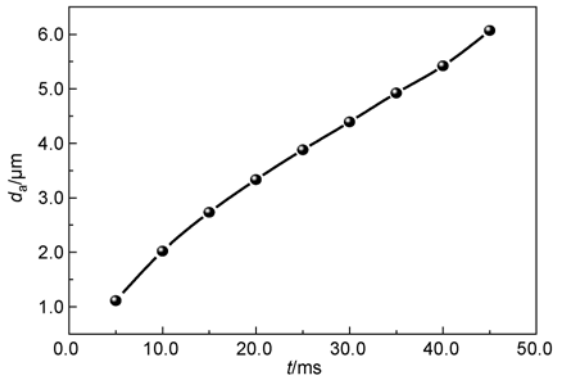

Figure 4 Surface layer thickness vs. phase separation time.

The droplet will automatically shrink into a sphere under the influence of surface tension, with the surface free energy considered. The alloy composition remains $(Ni_xCu_{100-x})_{50}Pb_{50}$. The fluidity parameter C_f=1000, and lattice sizes within the circular region are 300×300. The calculated results are shown in Figure 5. The snapshots of Figure 5(a) and (b) correspond to phase separation time of 16 ms and 32 ms. The black Pb-rich phase migrates preferentially to the surface, and the (Ni,Cu) phase depends on the Pb-rich phase to nucleate. The reason is that the surface tension of the Pb-rich phase is smaller than that of the Ni-rich phase. Accordingly, the state in which Pb-rich phase is located on the surface layer will be favorable for reducing total energy. With the extension of the phase separation time, the segregation layer gradually becomes thick. The (Ni,Cu) phase

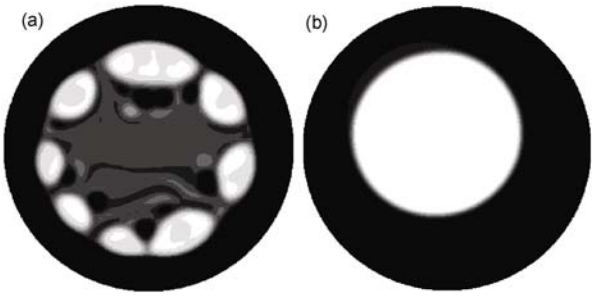

Figure 5 The influence of surface segregation on phase separation. Pb concentration ϕ_0=0.5 and fluidity parameter C_f=1000. The black part is the Pb-rich phase and the white part is the (Ni,Cu) phase. (a) and (b) are snapshots at 16 ms and 32 ms.

migrates to the central part, and then coagulates together, whereas the (Pb) phase aggregates at the surface. Afterwards, a two-layer core-shell microstructure is formed at 32 ms.

The calculated results show that the (Ni,Cu) phase is not located in the sphere center, but leans to one side, as shown in Figure 5(b). It is inferred that the fluid field plays an important role in the motion of the Ni-rich phase. In order to estimate the influence of the fluid field, the vectorgraph is illustrated in Figure 6, corresponding to 16 ms and 32 ms. Although the vector length of the flow field is large and the direction is various at 16 ms, the fluid field markedly reduces and becomes regular at 32 ms. The fluid field in the vicinity of the liquid-liquid interface is always strong. The solute diffusion is accelerated in the early stage and the fluid effect will subsequently decrease. A regular two-layer core-shell microstructure eventually forms.

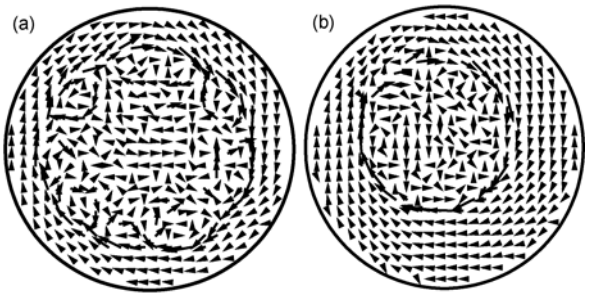

Figure 6 Fluid field distribution vs. time. (a) and (b) correspond to 16 ms and 32 ms.

The microstructures display distinct morphologies at different phase separation stages, and finally form a quasi-regular structure. In fact, due to the stirring of the fluid field, the thickness of the surface layer becomes uniform. Thus, the mean thickness d_a denotes the ratio of the Pb-rich phase area to circle length. The calculated results are similar to that in Figure 4. The thickness of the segregation layer apparently increases as the phase separation time extends.

Radial concentration distributions at different time are plotted in Figure 7, which corresponds to 12 ms, 20 ms, 28 ms and 36 ms. R=0 denotes the center of alloy melt. In the early stages of phase separation, the bulk concentration remains constant but surface concentration substantially fluctuates. In the late stages of phase separation, the concentrations of both the (Ni,Cu) phase and the Pb-rich phase remain constant with the entire system achieving a metastable state.

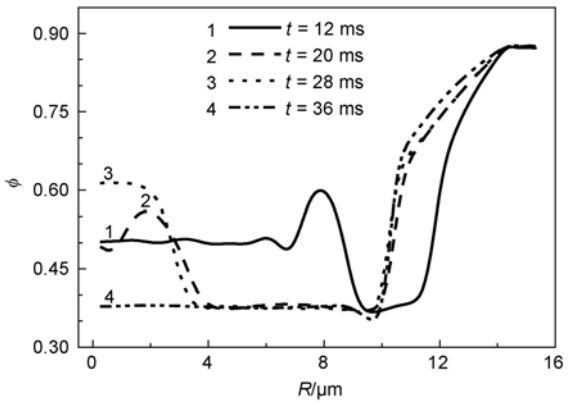

Figure 7 Variation of Pb concentration along a radial direction at different time.

The microstructural evolutionary process of ternary $(Ni_xCu_{100-x})_{50}Pb_{50}$ monotectic alloys was calculated by coupling the temperature field, fluid field and surface segregation. It is evident that surface segregation is a dominant factor for the formation of the surface layer, concentration profile variation and phase separation morphology. If the surface segregation is not incorporated, a two-layer core-shell microstructure is difficult to produce. The physical significance of surface segregation is not clear at present. Although most researchers describe it with a sophisticated form, illumination of physical significance of surface segregation remains essential. For example, an accurate function expression is necessary.

3 Conclusions

(i) The phase separation evolution was investigated using the phase field method, which incorporated the temperature field and the fluid field. If the surface segregation was not incorporated, the dynamic morphologies of alloy melt would show a transition from a disperse microstructure into a bicontinuous microstructure with the increase of the fluidity parameter.

(ii) Owing to the effect of surface segregation, the Pb-rich phase migrated preferentially to the surface of the liquid alloy, and the (Ni,Cu) phase nucleated depending on the Pb-rich phase. With the extension of the phase separation time, the thickness of the surface layer gradually increased. The (Ni,Cu) phase migrated and aggregated at the central part, and finally a two-layer core-shell microstructure was produced.

(iii) Under the influences of surface segregation, the surface concentration fluctuated more drastically than

that inside the bulk phase, and then transfered from the surface to the interior. The concentration in the bulk phase changed subsequently, and the concentration of both the (Ni,Cu) phase and the Pb-rich phase remained constant.

(iv) The fluid field in the vicinity of the liquid-liquid interface was strong and turbulent. The solute diffusion was facilitated, and the spatial symmetry was broken. The (Ni,Cu) phase was not located in the sphere center, but leaned to one side.

(v) The surface segregation was a crucial factor for the formation of the surface layer, concentration evolution and phase separation morphology. In the phase separation process of alloy melt, the surface segregation played an important role in the formation of the double-layer core-shell microstructure.

The authors are grateful to Prof. W J Xie, Mr. J Chang, Mr. C L Shen and Mr. L Chen for their suggestions.

1 Puri S, Binder K. Power laws and crossovers in off-critical surface-directed phase decomposition. Phys Rev Lett, 2001, 86(9): 1797－1800

2 Li J F, Cao Q P, Zhou Y H. Microstructure of $Cu_{60}Zr_{20}Ti_{20}$ bulk metallic glass rolled at different strain rates. Sci China Ser G-Phys Mech Astron, 2008, 51(4): 394－399

3 Tegze G, Pusztai T, Gránásy L. Phase field simulation of liquid phase separation with fluid flow. Mater Sci Eng A, 2005, 413-414: 418－422

4 Tanaka H. Wetting dynamics in a confined symmetric binary mixture undergoing phase separation. Phys Rev Lett, 1993, 70(8): 2770－2773

5 Bhagavatula R, Jasnow D. Phase asymmetry in thermocapillary motion. J Chem Phys, 1996, 105(1): 337－343

6 Huo Y L, Jiang X L, Zhang H D. Hydrodynamic effects on phase separation of mixtures with reversible chemical reaction. J Chem Phys, 2003, 118(21): 9830－9837

7 Hohenberg P C, Halperin B I. Theory of dynamic critical phenomena. Rev Mod Phys, 1977, 49: 435－479

8 Rane S S. Liquid-liquid phase separation in solutions of living semiflexible polymers. J Chem Phys, 2003, 118(1): 407－413

9 Bažec M, Žumer S. Simulation of phase separation of polymer-liquid-crystal mixtures and the effect of confining external surfaces. Phys Rev E, 2006, 73: 021703

10 Khan A. Liquid water model: Predicting phase separation and phase characteristics. J Mol Struct, 2005, 755: 161－167

11 Kim J. Numerical simulations of phase separation dynamics in a water-oil-surfactant system. J Colloid Interface Sci, 2006, 303: 272－279

12 Ni D, Shi H J, Yin Y J, et al. Dynamics of phase separation in mixed lipid membranes between two bounding walls. Physica B, 2007, 388: 159－166

13 Heijna M C R, Van Enckevort W J P, Vlieg E. Crystal growth in a three-phase system: Diffusion and liquid-liquid phase separation in lysozyme crystal growth. Phys Rev E, 2007, 76: 011604

14 Zhang X H, Ruan Y, Wang W L, et al. Rapid solidification and dendrite growth of ternary Fe-Sn-Ge and Cu-Pb-Ge monotectic alloys. Sci China Ser G-Phys Mech Astron, 2007, 50(4): 491－499

15 Dai F P, Cao C D, Wei B B. Phase separation and rapid solidification of liquid $Cu_{60}Fe_{30}Co_{10}$ ternary peritectic alloy. Sci China Ser G-Phys Mech Astron, 2007, 50(4): 509－518

16 Vladimirova N, Malagoli A, Mauri R. Two-dimensional model of phase separation in liquid binary mixture. Phys Rev E, 1999, 60(6): 6968－6977

17 Cahn J W, Hilliard J E. Free energy of a nonuniform system. I. Interfacial free energy. J Chem Phys, 1958, 28: 258－267

18 Qin T, Wang H P, Wei B B. Simulated evolution process of core-shell microstructures. Sci China Ser G-Phys Mech Astron, 2007, 50(4): 546－552